KOREL – User's guide

P. Hadrava

Astronomical Institute, Academy of Sciences of the Czech Republic,
251 65 Ondřejov, Czech Republic
e-mail: had@sunstel.asu.cas.cz
http://www.asu.cas.cz/˜had/korel.html

The code KOREL for Fourier disentangling (i.e. simultaneous decomposition of component spectra and solution of orbital elements) and 'line-photometry' of binary and multiple stars is described together with auxiliary codes PREKOR, KORNOR etc.

Keywords: Binary stars – spectroscopic, spectra disentangling

Contents

1   Introduction

KOREL is one of the software products developed by the present author for the data processing in the stellar department at Ondřejov observatory. It complements the codes SPEL (for solution of **sp**ectroscopic **el**ements of binary stars written by J. Horn) and FOTEL (P. Hadrava 1990, 1991, 2004) for **phot**ometric + spectroscopic **el**ements). In both these codes the orbital elements of binaries (or triple systems) are solved from radial velocity (RV- hereafter) curves, in the later case simultaneously with the solution of light-curves, visual (interferometric) measurements or eclipses timing.

To get RV-curves it is required to find and to identify at least some spectral lines belonging to individual component stars in different exposed spectra of the binary, to measure their observed wavelengths and to calculate their Doppler-shifts. This procedure is quite laborious, even if some handy tool like another Ondřejov code SPEFO (written by J. Horn, cf. P. Škoda 1996) is used. Moreover, if the line widths of one or more components are larger than the amplitude of the RV-curve, the lines are blended and the standard methods of measurement of the line centers are subjected to errors, or they cannot be used at all. This takes place in the vicinity of conjunctions even for sharp lines and the corresponding exposures are thus useless for solution of RV-curves.

The method of spectra disentangling, performed by the code KOREL, enables to overcome this problem. Comparing all available spectra obtained at different orbital phases, this method fits them as a superposition of some a priori unknown spectra attributed to individual components, each one Doppler shifted either for RV, which is a free parameter of the fit, or – even better – for RV, which corresponds to the orbital parameters solved directly without the unnecessary step of construction of RV-curve. The procedure is thus much easier even in the cases when the standard method via RV-curves can be applied. Moreover, the component spectra, which are obtained simultaneously with the orbital parameters, can be used for subsequent interpretation of the results, e.g. for determination of spectral types.

The mathematical method using Fourier transform (developed from the technique of cross-**cor**elation for RV-measurements to solve for the orbital **el**ements), which is employed in KOREL, enables further generalization for intrinsic line-profile variations (LPVs). In the first step this generalization involves changes of line strengths. This ability of KOREL was aimed originally to improve the fit of spectra obtained during a partial eclipse in the binary (the method of line-photometry). However, it yields an additional option, namely to decompose also the telluric lines.

In this document, the mathematical principle of the method is reviewed in Section 2. Some more details on the numerical method used in the code can be found in Section 3. The practical use of the code is described in Section 4.

The information (occasionally updated) about KOREL, including this document, is available on WWW at http://www.asu.cas.cz/~had/korel.html. The source files of the codes and some examples of their use can be downloaded by authorized users.[1]

2   Disentangling of composite spectra

2.1   Methods of radial-velocity measurements

2.1.1   Method of cross-correlation

The idea of this method is based on the fact that the presence of a weak signal of particular type, like is the spectrum of a faint secondary component, blended with a stronger signal or hidden in a noise can be better revealed from overall coincidence with the observed signal than from some local features (cf. Fig. 1). The Doppler shift of spectrum is constant in logarithmic wavelength scale

$$x = c \ln \lambda \tag{1}$$

and, in non-relativistic approximation ($v = c\Delta\lambda/\lambda = \Delta x$), linear in the radial velocity v. The cross-correlation

$$F(v) \equiv \int I(x+v)J(x)dx \tag{2}$$

of the observed spectrum $I(x)$ with a properly chosen template spectrum $J(x)$ thus indicates the velocity shifts at which a similar contribution appears in the spectrum (cf. e.g. Simkin 1973, Hill 1993).[2]

An ideal template J should contain the same lines in the same ratios of their strengths as the spectrum of component to be measured. In practice an observed spectrum of a star of similar spectral type or a synthetic spectrum from a model-atmosphere are used. Fortunately, experience shows that cross-correlation is not that sensitive to the choice of the spectral type of the template spectrum. Nevertheless, the template spectrum should be known a priori.

---

[1]The IP-address of computer(s) for which the access is requested should be sent (e.g. via the author's e-mail address given above in heading) to register and to get on the list of authorized users.

[2]The differences of the spectra from their continua are cross-correlated in practice to subtract large constants from the integral.
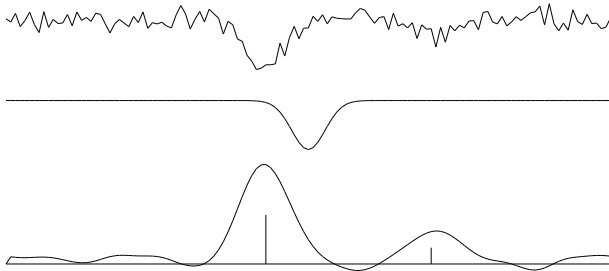
Fig. 1. Example of cross-correlation – synthetic spectrum constructed as a superposition of lines of two components and a noise (the upper curve) correlated with an ideal line-profile (middle spectrum) gives a curve with amplitudes and positions of local maxima corresponding to the strengths and RVs of lines of the components (marked by vertical abscissae at the bottom curve), while the noise is smeared out by the integration.

This can be quite difficult task to estimate for a faint companion.[3]

A generalization of this method is a two-dimensional cross-correlation

$$F(v_1, v_2) = \int I(x)[J_1(x - v_1) + J_2(x - v_2)]dx , \quad (3)$$

enabling to choose templates corresponding to different spectral types for the primary and secondary component (cf. Zucker and Mazeh 1994, Zucker et al. 1995).

Other shortcomings of the cross-correlation technique are the facts that the cross-correlation profile is broadened due to widths of both the observed spectrum and the template[4] and that some side-peaks may arise in the cross-correlation from coincidence of mutually non-corresponding lines in the observed spectrum and in the template.

2.1.2 Method of broadening function

The above mentioned shortcomings of cross-correlation method are well analyzed by Rucinski (2002), who introduced a method of broadening function (Rucinski 1992) to overcome them. In this method, the broadening function $B(x)$ is calculated to satisfy the relation

$$I = B * J \quad (4)$$

between the template and the observed spectrum. If the observed spectrum corresponds to a Doppler-shifted template or to a superposition of them for each component, then B is a shifted Dirac delta-function, or a sum of them. One or more components may also correspond to a broadened template spectrum (e.g.

due to a rotation broadening). In favourable cases when lines of I are wide and lines of J are narrow, B will be a Doppler shifted broadening profile. For a given I and chosen J, Eq. (4) can be solved with respect to B using e.g. the method of singular-value decomposition. Position of peak of B gives again the information about the instantaneous Doppler-shift of the observed spectrum. The shape and especially the width of peak of B, which unlike F in Eq. (2) is not quadratic in the line profile, can yield also an information about the broadening of lines in I. However, the problem of the proper choice of the template is still opened in this method and, at least equally important as in the method of cross-correlation.

2.2 Methods of decomposition of spectra

2.2.1 Direct decomposition

It is important to distinguish contributions of individual components of a multiple stellar system to its common spectrum not only to be able to measure the RVs and to solve for orbital parameters, but also to find the physical characteristics of atmospheres of the stars and to put them into context with their masses and evolutionary status. An exceptional opportunity is yielded by eclipsing binaries for which spectrum of one component can be obtained during a total eclipse and the other spectrum can be found as its difference from spectrum obtained out of eclipse. However, for majority of stellar systems some more sophisticated methods must be used. The most straightforward of them is the method of direct subtraction involved by Ferluga et al. (1991, 1997), in which two spectra I_a, I_b of a binary obtained at different phases (best of all at the opposite elongations, at extremes of RVs $v_{a,b}$ of both components) are used. If the spectra of individual components are J_1, J_2, the relation

$$I_a(x) = J_1(x - v_{1a}) + J_2(x - v_{2a}) , \quad (5)$$
$$I_b(x) = J_1(x - v_{1b}) + J_2(x - v_{2b}) , \quad (6)$$

---

[3]The initial motivation for Fourier disentangling was an attempt to overcome this problem using a kind of cross-correlation of spectra of the same binary obtained at different phases.

[4]Spectra of stars with small rotational $v \sin i$ are thus preferable templates and attempts to make them more similar to the spectra of measured components by numerical rotational broadening spoil the information offered by the final cross-correlation.

should be valid. From here we can calculate both spectra recurrently

$$
\begin{aligned}
J_1(x) &= J_1(x - v_{1a} + v_{1b} + v_{2a} - v_{2b}) - && (7) \\
&\quad - I_a(x + v_{1b} + v_{2a} - v_{2b}) + I_b(x + v_{1b}) , \\
J_2(x) &= J_2(x - v_{1a} + v_{1b} + v_{2a} - v_{2b}) + && (8) \\
&\quad + I_a(x + v_{2a}) - I_b(x - v_{1a} + v_{1b} + v_{2a}) ,
\end{aligned}
$$

starting from a wavelength, where the spectra of both components can be approximated by continuum, and proceeding in positive or negative direction of the logarithmic wavelength variable x (depending on the sign of the expression $v_{1a} - v_{1b} - v_{2a} + v_{2b}$) toward groups of spectral lines.

This straightforward method clearly shows an obstacle, which is in principle a problem also for later more sophisticated methods. The region of values of x covered by each exposure contains information about spectra of individual components in regions shifted for $v_{1,2}$, so that the information on both spectra is available only in the overlap of both regions. To be able to separate both spectra, one must add the missing information about the spectrum of the other component, usually the assumption that it is a pure continuum without any line. However, this can be a source of error, which may then spread also inside the region where the solution should be well determined.

The main disadvantage of this method is the fact, that owing to the recurrent procedure of solution the influence of random observational noise (which should be added on the right-hand sides of Eqs. (5) and (6)) is cumulative, so that after passing a group of spectral lines the solution can deflect from the correct value of the continuum. The influence of the noise can be reduced by averaging results of solutions obtained from a larger number of pairs of exposures. However, this suggests to develop a method searching ab initio for the best fit to a higher number of observed spectra, so that the solution $J_{1,2}$ of corresponding system of linear equations of type (5) would be overdetermined.

2.2.2 Method of tomographic separation

A method for decomposition of a larger number of observed spectra of a binary (with known RVs) was introduced by Bagnuolo and Gies (1991). Their method is based on the mathematical equivalence of this task with the problem of image reconstruction in tomography. The superposition of Doppler-shifted component spectra at different orbital phases can be treated as projection of two parallel linear objects (e.g. photographic spectrograms) viewed from different angles. Any standard numerical method of tomographic reconstruction should thus be able to calculate the distribution of intensities (or opacities) in this object of dimension $2 \times N$ from a higher number of exposures

(each one consisting typically of N pixels) if a sufficient coverage of viewing angles / orbital phases is available – cf. Fig. 2.[5]

The observational noise in individual exposures can thus be diminished by the averaging tendency of this method. The disadvantage of needing to know the RVs first is common for both mentioned methods of decomposition. However, complementing this approach with the method of cross-correlation, it is obvious that both the decomposition of the spectra and the measurement of RVs (and solution of orbital parameters) should be possible in an iterative process, without the ad hoc choice of the template spectrum.

2.3 Method of simple disentangling of spectra

The first method enabling simultaneous decomposition of the spectra of binaries and measurement of their RVs, or actually directly the solution of orbital parameters was published by Simon and Sturm (1994).[6]

The decomposition of the spectra is solved by Simon and Sturm (similarly as in the methods by Ferluga or Bagnuolo and Gies) directly for $2M$ values of spectral fluxes $\mathbf{I}_A$ and $\mathbf{I}_B$ of components A and B at individual values of the independent variable x (here M corresponds to the number of pixels in the typical exposure which is typically of the order 10^3). A set of $N \times M$ linear equations

$$
\begin{pmatrix}
\mathbf{M}_{A1} & \mathbf{M}_{B1} \\
& \ldots & \\
\mathbf{M}_{AN} & \mathbf{M}_{BN}
\end{pmatrix}
\begin{pmatrix}
\mathbf{I}_A \\
\mathbf{I}_B
\end{pmatrix}
=
\begin{pmatrix}
\mathbf{I}(t_1) \\
\ldots \\
\mathbf{I}(t_N)
\end{pmatrix} , \quad (9)
$$

is obtained for these unknown values, where N is the number of exposures (it must be $N \geq 2$). There are N subvectors $\mathbf{I}(t_l)$ of dimension M with spectra observed at times $t_l|_{l=1}^N$ of exposures on the right-hand side of this equation. The submatrices

$$
\mathbf{M}_{jl} =
\begin{pmatrix}
0 & \ldots & 1 & & \ldots & \\
& 0 & & 1 & & \\
& & \ldots & & & \\
\ldots & & 0 & \ldots & 1 \\
& & \ldots & & & \\
& \ldots & & & 0 &
\end{pmatrix}
\qquad (10)
$$

overbrace label: $v_j(t_l)$

of dimension $M \times M$ on the left-hand side have the only nonzero elements equal to 1 shifted from the

---

[5] The equivalence of both mathematical problems can be used also in the opposite direction, it means that numerical methods for spectra decomposition could be applied for computer tomography as well (cf. Hadrava 2001a).

[6] They also introduced for their method the name 'disentangling', which is used here to denote the problem in this complexity.
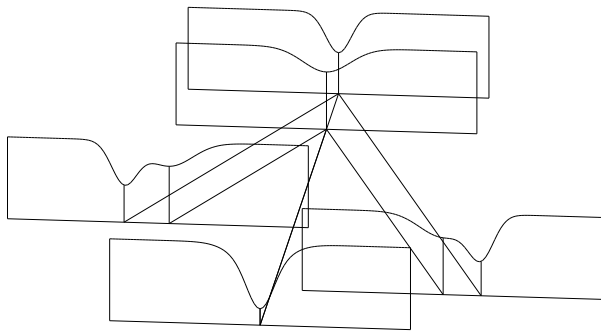
Fig. 2. Principle of tomographic separation – projections of spectra of individual components (the two spectra in the back) into different directions correspond to different Doppler shifts in different phases (the three spectra in the foreground).

main diagonal for a number of pixels corresponding to the values $v_j(t_l)$ of Doppler shift of component $j|_{j=A}^{B}$ at time t_l. Simon and Sturm solved this set of equations which has a sparse matrix but of very high dimension using the method of 'singular value decomposition'. This method has been applied on real data in several studies (e.g. Sturm and Simon 1994, or Simon et al. 1994). It could be mentioned that the method was tested also by Hynes and Maxted (1998) using some simulated data.

Despite the fact that the decomposition of the spectra is the more difficult part of the disentangling, including the solution of orbital parameters into the same procedure represents an essential qualitative advance in the interpretation of the stellar spectra. An ideal procedure of any interpretation would be to fit the observational data by a complete theoretical model and to estimate, how far the conclusions of the study are determined by the original observations. If this task is split into subsequent steps like the determination of RVs in individual exposures first and the solution of RV-curves only after, the information about the decisive power of the source data is partly lost in the questionable reliability of the intermediate results. This is a reason to prefer the direct solution of orbital parameters instead of disentangling of component spectra together with their RVs[7] and the same strategy leads us to consider a further generalization of the method of disentangling to include simultaneously some other effects, like the line-profile variability. At the same time, the user must be aware that the choice of a particular model to fit the data may be biased and even good results do not exclude that some other model may better explain the same data or data enriched by some additional observations.

---

[7]Such an option may be preferable if the spectra contain a component which need not follow any orbital motion, like an absorption in gaseous streams projected on photospheres of components in interacting binaries.

2.4 Fourier disentangling and its generalizations

Unlike the approach by Simon and Sturm, which is based on the decomposition of spectra in the wavelength domain, KOREL uses the least square fit of Fourier transforms of observed spectra (Hadrava 1995, cf. Section 2.4.1), which makes the solution numerically easier and which thus enables further generalizations (see e.g. Hadrava 1997, 2004a and Sections 2.4.3 and 2.4.5). The mathematical basis of the present method is analogous to the cross-correlation technique, however, the basic difference from the standard cross-correlation (e.g. Hill 1993) or its two-dimensional generalization (Zucker and Mazeh 1994) is that in KOREL all spectra at different phases of the same variable star are mutually compared and decomposed instead of performing cross-correlation of each spectrum of the variable separately with an ad hoc chosen standard. Numerous applications of this method to real data have been recently reviwed by Holmgren (2004).

2.4.1 Principle of Fourier disentangling

Let us suppose that a multiple stellar system consists of n stars and that the spectrum $I_j(x)|_{j=1}^{n}$ of each component is constant in time (i.e. it has no intrinsic physical or geometric variability) apart of being Doppler shifted according to the instantaneous radial velocity $v_j(t)$ of the star j at the time t. The composite spectrum observed at time t can be then expressed as a sum of convolutions (in the logarithmic wavelength-scale given by Eq. (1)) with correspondingly shifted Dirac delta-functions,

$$I(x,t) = \sum_{j=1}^{n} I_j(x) * \delta(x - v_j(t)) . \qquad (11)$$

Comparing such spectra obtained at different times, we would like to find what is the same for all of them, i.e. the spectra $I_j(x)$ of the components, and what is changing, i.e. the instantaneous RVs $v_j(t)$. This is in principle possible if we have more than n spectra obtained at different RVs. Assuming the RVs to

be known, this huge set of linear equations can be solved with respect to $I_j(x)$ and the observed spectra can thus be decomposed. The experience from the cross-correlation method shows, that it is numerically advantageous to treat Eq. (2) also as a convolution (taking appropriate inversions of the involved functions) and to perform its calculation by Fourier transform. In the problem of spectra decomposition the Fourier transform $(x \rightarrow y)$ of Eq. (11) reads

$$\tilde{I}(y,t) = \sum_{j=1}^{n} \tilde{I}_j(y) \exp(iyv_j(t)) , \qquad (12)$$

i.e. it simplifies the task essentially, because the huge set of linear equations splits now into many simple systems of dimension equal to the number of components in the observed system. The solution is similar to quantum mechanics, where any linear operator can be equivalently written in different representations, however, it is easier to calculate its functions and in particular its inversion in a reducible representation. This is the basic trick which makes the Fourier disentangling more versatile compared to the wavelength domain disentangling, despite in principle both methods are equivalent and their general features, which are easier to understand in one representation are in fact valid for the other as well.[8]

Before explaining the procedure of solution of Eqs. (11) or (12), let us generalize them for purposes of later development of the method. In view of the possibility to involve a broadening of line-profiles similarly as the Doppler shifts by another convolution with a corresponding broadening profile (cf. Eq. (4)), we can generalize Eq. (11) to

$$I(x,t) = \sum_{j=1}^{n} I_j(x) * \Delta_j(x,t,p) , \qquad (13)$$

and its Fourier transform to

$$\tilde{I}(y,t) = \sum_{j=1}^{n} \tilde{I}_j(y) \, \tilde{\Delta}_j(y,t,p) , \qquad (14)$$

where Δ_j are some general broadening functions, which may involve now not only the Doppler shifts, but possibly also some line-profile broadenings at the time t; $\tilde{\Delta}_j$ are their Fourier transforms. These functions depend on some parameters p characterizing either the

---

[8]It is obvious that for the special case $n = 2$, Eqs. (11) or (12) are equivalent with Eq. (9). Consequently, it is incorrect, what Simon and Sturm (1994, p. 291) claim, that unlike the problem of tomography, which is analytical by its nature, the decomposition or disentangling is the algebraic one. Both these problems, as well as others related with them, can be formulated analytically and solved algebraically in a chosen numerical representation. The generalizations of disentangling given below could be, in principle, done also in the wavelength domain as it was done in the pioneering work by Simon and Sturm. However, the numerical solution would be then more difficult.

orbital motions of the components or physical and geometric conditions of formation of their spectra.

The principle of disentangling consists in minimization of the sum of integrated squares of differences between the observed and model spectra (on the left and right hand sides of Eq. (13), respectively)

$$0 = \delta \sum_{l=1}^{N} \int \left| I(x,t_l) - \sum_{j=1}^{n} I_j(x) * \Delta_j(x,t_l,p) \right|^2 dx, (15)$$

which is supposed to be due to observational noise in $I(x,t)$. This expression implicitly assumes, that the noise is the same for all wavelengths. Only limited spectral regions are available in practice, which means that outside the corresponding range of x we take the spectra with zero weight. The minimization is performed with respect to the component spectra $I_j(x)$ (which gives the decomposition of the spectra) as well as to the orbital parameters (corresponding to the solution of RV-curves with implicitly involved RV measurements) or other free parameters p.

According to the Parseval theorem, the norm of a function is proportional to the norm of its Fourier transform

$$\begin{aligned} \int |\tilde{f}(y)|^2 dy &= \int \tilde{f}^*(y) \int \exp(ixy)f(x)dxdy = \\ &= \int f(x) \left[\int \tilde{f}(y) \exp(-ixy)dy \right]^* dx = \\ &= 2\pi \int |f(x)|^2 dx , \qquad (16) \end{aligned}$$

where the asterisk $*$ denotes complex conjugate. Consequently, the condition (15) can be equivalently rewritten as minimization (i.e. zero variation) of sum of integrals of the Fourier transforms

$$0 = \delta \sum_{l=1}^{N} \int \left| \tilde{I}(y,t_l) - \sum_{j=1}^{n} \tilde{I}_j(y)\tilde{\Delta}_j(y,t_l,p) \right|^2 dy . \ (17)$$

This form of the condition assumes implicitly, that the noise is white, which need not be always the case, as we shall discuss later. It can thus be better to involve some weights $w_l(y)$ of individual Fourier modes and to write the condition in the form

$$0 = \delta S , \qquad (18)$$

where

$$\begin{aligned} S &= \qquad\qquad\qquad\qquad\qquad\qquad (19) \\ &= \sum_{l=1}^{N} \int \left| \tilde{I}(y,t_l) - \sum_{j=1}^{n} \tilde{I}_j(y)\tilde{\Delta}_j(y,t_l,p) \right|^2 w_l(y)dy . \end{aligned}$$

The equation for decomposition of spectra can be obtained by varying S with respect to individual Fou-

rier modes,[9]

$$0 = \frac{\partial S}{\partial \tilde{I}_m^*(y)} = \qquad (20)$$

$$= -\sum_{l=1}^{N} \left[\tilde{I}(y, t_l) - \sum_{j=1}^{n} \tilde{I}_j(y) \tilde{\Delta}_j(y, t_l, p) \right]$$
$$. \tilde{\Delta}_m^*(y, t_l, p) w_l(y) =$$

$$= \sum_{j=1}^{n} \left[\sum_{l=1}^{N} \tilde{\Delta}_j(y, t_l, p) \tilde{\Delta}_m^*(y, t_l, p) w_l(y) \right] \tilde{I}_j(y) -$$
$$- \sum_{l=1}^{N} \tilde{I}(y, t_l) \tilde{\Delta}_m^*(y, t_l, p) w_l(y) ,$$

which is obviously a set of n linear equations for each Fourier mode separately. To optimize the solution with respect to the parameters p we can use the conditions

$$0 = \frac{\partial S}{\partial p} = \qquad (21)$$

$$= -2\Re \sum_{l=1}^{N} \int \left[\tilde{I}(y, t_l) - \sum_{j=1}^{n} \tilde{I}_j(y) \tilde{\Delta}_j(y, t_l, p) \right]$$
$$. \sum_{m=1}^{n} \tilde{I}_m^*(y) \frac{\partial \tilde{\Delta}_m^*(y, t_l, p)}{\partial p} w_l(y) dy .$$

However, the dependence of $\tilde{\Delta}_j$ on p can be generally quite complicated and consequently also the solution of these equations may be difficult. It can thus be easier to minimize directly the expression for S in the form (19) using some numerical method of optimization, like the simplex method.

Let us note that despite the determination of RVs and subsequent solution of RV-curve is an obsolete procedure compared to the disentangling of spectra, it may be still useful to determine RVs for individual exposures first to enable their combination with older data from literature or with solution of light-curves. Having already disentangled a set of spectra, it is possible to measure RVs of the component stars in each of them by fitting the spectrum as a superposition of the disentangled spectra Doppler-shifted for velocities independent of the found orbital parameters.

2.4.2 Simple Fourier disentangling

Let us illustrate the Fourier disentangling first in the simple case, which is equivalent to the above explained method by Simon and Sturm (cf. Section 2.3), with the only generalization that the observed system need

not be a binary only, but it may consist of n stars. Then Δ-functions corresponding to the pure Doppler shifts are given by

$$\Delta_j(x, t_l, p) = \delta(x - v_j(t_l, p)) , \qquad (22)$$

their Fourier transforms are

$$\tilde{\Delta}_j(y, t_l, p) = e_{jl} \equiv \exp(iyv_j(t_l, p)) , \qquad (23)$$

and consequently (if we skip the weights $w_l(y)$ for simplicity) Eq. (20) reads

$$\sum_{j=1}^{n} \left[\sum_{l=1}^{N} e_{jl} e_{ml}^* \right] \tilde{I}_j(y) = \sum_{l=1}^{N} e_{ml}^* \tilde{I}(y, t_l) . \qquad (24)$$

This set of equations can be solved with respect to $\tilde{I}_j(y)$ whenever the matrix (with indices j, m) on the left-hand side is non-singular.

It is obvious that the singularity occurs always for $y = 0$ (which can be seen also in Eq. (12)), when this equation reduces for all m to a single condition

$$\sum_{j=1}^{n} \tilde{I}_j(0) = \frac{1}{N} \sum_{l=1}^{N} \tilde{I}(0, t_l) \qquad (25)$$

for the sum of mean values of the component spectra to give the mean value of the observed spectra. It means, that the continua cannot be directly decomposed, because they are not influenced by the Doppler shifts. An indirect method of distinguishing the contributions to the continuum is described in Section 2.4.4. This problem will be discussed in detail in Section 2.5. It can happen also for non-zero Fourier modes that the matrix is nearly singular and the solution is thus unstable. This danger is higher for low modes, for which the Doppler effect is smaller. These modes can be more influenced by errors in rectification of spectra. This is why it may be better to filter them out using some weights $w_l(y)$ as additional multiplicators in the integrals in expression (19). These multiplicators will not influence the decomposed spectra directly by the amplitudes and phases of individual Fourier modes but through the optimal values of the parameters p. It is possible in KOREL to cut out a chosen number of lowest modes.[10]

As mentioned in the previous Section, limited ranges with a finite sampling are used in practice both in the wavelength domain as well as in the domain of Fourier transforms of spectra. The highest efficiency of numerical calculation is achieved if the numbers

---

[9]Because $\tilde{I}$ are complex values, the partial derivatives of S must be calculated either independently with respect to their real and imaginary parts, or with respect to $\tilde{I}$ and its complex conjugate as independent variables.

[10]Ilijić et al. (2000) advocate a filtering of high frequency noise from spectra before the disentangling. It would be possible to involve the filtering directly into the procedure of disentangling, if such a need will be confirmed. The present version of KOREL does not allow it not to complicate much its use. Some filtering of high frequencies is performed already by the interpolation of the original data into the chosen scale of x.

of bins in both representations are comparable. The Fourier transform between these limited sets of discretized data points assumes a periodic repeating. It means that a spectral line which disappears at some phase behind one edge of the spectral region to be decomposed is expected to appear at the other. Because this will not generally happen (unless by chance a similar line exists at the other edge), solution of decomposition cannot fit at the edges all observed spectra with and without the line. This leads to errors propagating from edges toward the middle of the decomposed range, as described by Ilijić et al. (2000). To prevent these errors the spectral regions chosen for the disentangling should have continua[11] without spectral lines at both edges of the decomposed spectral range, best of all wider than the expected amplitude of RVs of the components. To facilitate the choice of convenient spectral range code PREKOR has been written, which interpolates from the data-files with individual exposures into chosen regions with proper discretization and displays the result to enable a visual check of the input data for KOREL. It may be difficult to satisfy the demand for pure continua at edges of the region when disentangling is applied to late-type stars. In such a case the edge defects can be partly suppressed by the so called tapering of the signal towards the edges (or the hemming of signal window), i.e. a smooth suppressing the signal of source data in narrow strips on both edges towards the continuum, as it is recommended also in the technique of cross-correlation. This trick is in fact similar to the choice of slightly higher dimension of decomposed vectors $\mathbf{I}_{A,B}$ on the left-hand side of Eq. (9) of the method by Simon and Sturm than is the dimension of the source data $\mathbf{I}(t_l)$ on the right-hand side.

2.4.3 Line-strength variations and removal of telluric lines

The simplest generalization of the disentangling is to abandon the assumption of constant component spectra and to admit a change of strength of lines of some component. The original motivation for this step was the experience that in some binaries errors of RVs increased significantly close to conjunctions where an eclipse could be expected. If the contribution of one eclipsed star is missing in the spectrum of the whole system, the spectra of the remaining are more pronounced and their sum cannot be fitted so well as a superposition of lines with the same depths as out of the eclipse.

Let us thus generalize Eqs. (22) and (23) by involv-

ing time-variable multiplicative line-strength factors $s_{jl} = s_j(t_l)$ for each component star, i.e.

$$\Delta_j(x, t_l, p) = s_{jl}\delta(x - v_j(t_l, p)) , \qquad (26)$$

the Fourier transforms of which read

$$\tilde{\Delta}_j(y, t_l, p) = s_{jl}e_{jl} . \qquad (27)$$

In this case Eq. (20) gets slightly more complicated form compared to (24), namely

$$\sum_{j=1}^{n}\left[\sum_{l=1}^{N}w_{l,X}(y)s_{jl}e_{jl}s_{ml}e_{ml}^{*}\right]\tilde{I}_{X,j}(y) =$$
$$= \sum_{l=1}^{N}w_{l,X}(y)s_{ml}e_{ml}^{*}\tilde{I}_X(y,t_l) \qquad (28)$$

Here the subscript X refers to different regions of the observed spectra, each one being characterized by its initial wavelength x and its dispersion (in the value of RV per one bin of the sampling in x). The weights $w_{l,X}(y)$ could be, in principle, different for each Fourier mode y in each spectral region X of the exposure l. However, in the present version of KO-REL, we choose[12]

$$w_{l,X}(y) = w_{l,X}w(y) . \qquad (29)$$

The weight $w_{l,X}$ of each exposure can be chosen, e.g., in dependence on the number of photon counts. The spectral filter $w(y)$ enables to cut out the lowest Fourier modes, as mentioned at the note [10] on page 21.

Following (27), S given by (19) is bilinear also in coefficients s_{jl}. Hence, varying with respect to s_{ml}, we get from Eq. (21) for each chosen exposure l the following set of linear equations

$$\sum_{j=1}^{n}\Re\left[\sum_{X}\int w_{l,X}(y)\tilde{I}_{X,j}(y)\tilde{I}_{X,m}^{*}(y)e_{jl}e_{ml}^{*}dy\right]s_{jl} =$$
$$= \Re\sum_{X}\int w_{l,X}(y)\tilde{I}_X(y,t_l)\tilde{I}_{X,m}^{*}(y)e_{ml}^{*}dy \qquad (30)$$

for these coefficients corresponding to different components. It is obvious from Eqs. (14) and (27) that for each component its spectrum $\tilde{I}_j(y)$ and strengths s_{jl} are defined by the observations up to a reciprocal multiplicator. This must be fixed by a normalization condition.

If strengths of some components are fixed, their terms must be transferred from the left- to the right-hand side of this equation. Because the coefficients s_{jl}

---

[11]Naturally the continua on both edges of each spectral region should have the same level to prevent also a discontinuity in jump between the edges of decomposed spectra. This can be ensured by the rectification of input spectra to their continua.

[12]The weights $w_{l,X}$ are part of input data for KOREL. They can be chosen before running PREKOR and altered for selection of different regions X if these are merged from different runs of PREKOR. The filter $w(y)$ is taken as the same function of the order of Fourier harmonic for all l, X which means that its scale in wavelengths of the original spectra is dependent on sampling in X.

are generally still quite numerous (but less in number than the Fourier modes of the component spectra), it is advantageous to solve for them directly from equations (30) before optimizing S with respect to either $v_j(t_l)$ or p, in which it is non-linear.

It is important to hold in mind that the solutions of orbital elements (or individual independent radial velocities), the decomposition of the spectrum and the solution of component strengths are inter-related and their self-consistent solution should be found. To find this solution, an iterative procedure is used if all these kinds of unknowns are allowed to converge. However, there is no guaranty that this scheme will converge from every arbitrarily chosen initial condition. Instead, it can achieve some false local minimum by suppressing lines in exposures for which true RVs differ from the instantaneous approximation or orbital parameters. It is thus often more efficient to approximate the solution of spectra and orbital parameters with fixed strengths (either found in some other spectral region, where lines of given components are better pronounced, or simply let them equal to one) first and to allow them to converge for a final tuning of the solution only.

The option of line strength solution enables a decomposition of the telluric lines (or, in principle, also some interstellar lines) from the observed spectra. Exactly speaking, the telluric component of the spectrum is not additive, but multiplicative, because the observed spectrum

$$I_{obs}(x,t) = \exp(-\tau(x,t))I_0(x,t) \qquad (31)$$

is proportional to the true composed spectrum I_0 of the studied stellar system as seen outside the Earth's atmosphere. However, this formula can be approximated as

$$I_{obs}(x,t) = I_0(x,t) + I_{tell}(x,t) , \qquad (32)$$

where telluric spectrum

$$
\begin{aligned}
I_{tell}(x,t) &= (e^{-\tau(x,t)} - 1)I_0(x,t) \simeq \\
&\simeq -\tau(x,t)I_0(x,t)
\end{aligned}
\qquad (33)
$$

is a negative contribution in lines with no continuum.[13] The optical depth τ and hence also strength of telluric lines is very sensitive to the air-mass and humidity at each exposure. Because usually we are not interested in the true telluric spectrum $\tau(x,t)$ but only in how to eliminate its influence, we can decompose its lines traveling with the annual motion of the Earth as they are imprinted on the mean $I_0(x)$. A small discrepancy may arise only with telluric lines falling on steep slopes of line profiles in $I_0(x)$, the strength of which in ratio to the strengths of lines falling to continuum of $I_0(x)$ can differ in each exposure depending on the instantaneous radial velocities.

---

[13]The small telluric absorption in continuum is eliminated by the rectification of the observed spectra.

2.4.4 Line photometry

Taking into account the connection between formation of continuum and spectral lines in stellar atmospheres, the above described method for calculation of line-strength variations yields a possibility to find differential magnitude changes between the components and also to determine the ratio of component continua in the case that the intensity variations are caused by some overall darkening of a component e.g. by an eclipse. Let in the 'normal' state of a binary (i.e. out of eclipse) the intensities $I_{1,2}$ of components continua be normalized

$$I_1 + I_2 = 1 . \qquad (34)$$

The line depths $L_{1,2}$ of the components found by solution of Eq. (28) are expressed in units of this common continuum with respect to which the input spectra were rectified. If in another exposure the spectrum of component '1' is decreased by factor $z\times$ (see Fig. 3), then the decomposed line depths of both components referred to the instantaneous common continuum will be changed by factors $s_{1,2}$ to values

$$s_1 L_1 = \frac{z_{lin}L_1}{z_{cont}I_1 + I_2} \qquad (35)$$

$$s_2 L_2 = \frac{L_2}{z_{cont}I_1 + I_2} . \qquad (36)$$

The factor z_{lin} can thus be simply expressed as

$$z_{lin} = \frac{s_1}{s_2} , \qquad (37)$$

and assuming that the factor z in continuum is the same, $z_{cont} \equiv z_{lin}$, the ratio of continua intensities can be also found as

$$\frac{I_1}{I_2} = \frac{1 - s_2}{s_1 - 1} . \qquad (38)$$

Obviously, if $z < 1$, then $s_1 < 1$ and $s_2 > 1$. This behavior can help to distinguish the variations caused by the 'geometrical' reasons (or their equivalent) from intrinsic variations of line intensities of a component or from the observational noise.

In the usual case of N exposures, the factors $z_l|_{l=1}^N$ of the darkenings of the component '1' can be calculated independently for each exposure from s_{jl} according to Eq. (37). The ratio of continua intensities can be then obtained by least square fit of Eqs. (35) and (36) e.g. in logarithmic (i.e. magnitude) scale, i.e. by solving the condition

$$0 = \delta \sum_l \left[\ln s_{2l} + \ln(1 + I_1(z_l - 1))\right]^2 \qquad (39)$$

for the variation δI_1.

The applicability of this simple estimate of ratio of continua from line photometry is limited by the
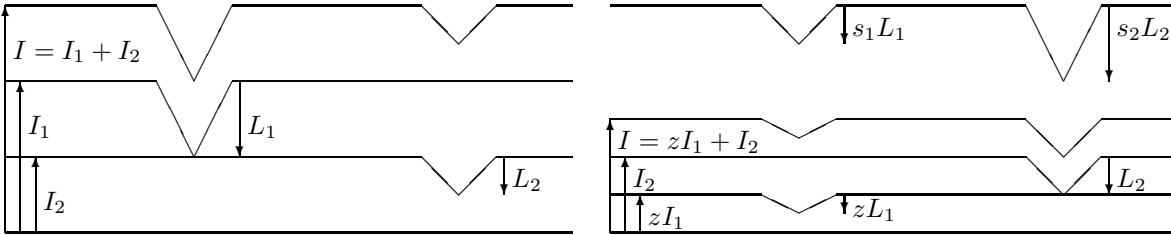
Fig. 3. Continuum and line strengths of uneclipsed components (left) and in the primary eclipse (right).

above mentioned assumption that the change of intensity is the same for the line and the continuum and certainly also by assumption that only two components are present as well as that there are no intrinsic changes of line profile shapes. Practical experience indicated that this is not exactly true even for eclipsing binaries, not to speak about stars where intrinsic line-profile variability can be expected due to ellipticity, radial or non-radial pulsations, spots or reflection. The reason can be simply understood in terms of limb-darkening variations within the line-profile. If the limb darkening is different in line and in continuum, the portions z of eclipsed light in numerator and denominator in Eq. (35) are different and cannot be solved together with $I_{1,2}$ from $s_{1,2}$, unless their relation is known from theory. On the other hand, fitting of $s_{1,2}$ by a more detailed model of eclipse light-curves in each x can reveal the limb-darkening variations within the line and thus yield information about the structure of atmosphere of the eclipsed component.

As shown in a preliminary study of this problem (Hadrava and Kubát, 2003), the variations of line profile across the stellar disk are generally very complex, so that even the often used expression of rotational broadening as a convolution with some rotational profile is in fact wrong. However, some relatively good approximations can be developed from the theory of stellar atmospheres, which will simplify the task to a solvable and quite powerful method.

If source-function in a plane-parallel atmosphere can be expanded into a Taylor-series in monochromatic optical depth

$$S(x,\tau) = \sum_k \frac{1}{k!} S_k(x)\tau^k \ , \qquad (40)$$

the surface intensity is polynomial in directional cosine μ with coefficients S_k,

$$I(x,\mu)|_{\tau=0} = \sum_k S_k(x)\mu^k \ . \qquad (41)$$

In the Milne-Eddington approximation these sums reduce to the first two terms, so that the distribution of intensity over the visible stellar disk

$$I(x,\mu)|_{\tau=0} \;=\; S_0(x) + S_1\mu = \qquad (42)$$

$$=\; I(x,1)|_{\tau=0}(1 - u + u\mu)$$

corresponds to linear limb darkening

$$u = \frac{S_1}{S_0 + S_1} \ , \qquad (43)$$

which is according the theory $u = \frac{3}{5}$ for the light integrated in frequencies and according to solutions of observed light-curves around $u \simeq 0.3$ for the visible light in wide frequency bands, i.e. in continuum.

Suppose that in all geometric depths (radii of the star r) the monochromatic opacity across a line-profile is proportional to the opacity in continuum with the same line-profile function ϕ dependent on the frequency x only.[14] Then also the monochromatic optical depth τ is proportional to the optical depth in continuum,

$$\tau(x,r) = [1 + \phi(x)]\tau_{cont}(r) \ . \qquad (44)$$

If conditions of LTE are satisfied for studied lines, S is a smooth (Planckian) function of x, so that its change within the line profile can be neglected and its slope in monochromatic optical depth varies only due to the opacity profile, $S_1(x)[1 + \phi(x)] \simeq S_{1,cont}$. The linear limb-darkening is thus decreasing toward the center of line

$$I(x,\mu)|_{\tau=0} = S_{0,cont} + S_{1,cont}[1 + \phi(x)]^{-1}\mu \ , \qquad (45)$$

and the line-contribution to the spectrum

$$[I(x,\mu) - I_{cont}(\mu)]_{\tau=0} = -S_{1,cont}\frac{\phi(x)}{1 + \phi(x)}\mu \ , \qquad (46)$$

which is negative, has distribution over the stellar disk corresponding to limb-darkening

$$u_{lin} = 1 \ . \qquad (47)$$

It means that at initial phases of an eclipse when only a part of disk edge is hidden, the light missing in line represents larger portion of the overall flux in that frequency than the light missing in the continuum

----

[14]This is not true generally. However, we can take the assumption of separability in variables r and x as the first approximation at least in a small region where the core of the line is formed.
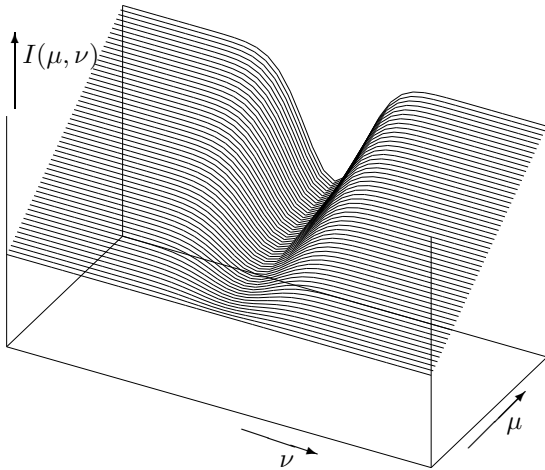
Fig. 4. Schematic dependence of limb darkening across line-profile of an absorption line. Intensity is low on edge of stellar disk ($\mu = 0$) both in continuum and the line, but it is more brightened toward the disk centre ($\mu = 1$) in continuum than in the line, because the radially escaping photons in continuum originate in deeper and hotter layers of the atmosphere. The central parts thus contribute to the formation of spectral lines with increasing weight.

($z_{lin} < z_{cont}$), so that in some cases line-strengths of both components can be enhanced. The z-factors from Eqs. (35) and (36) for an eclipse must be thus modelled simultaneously for the continuum and lines with their corresponding limb-darkenings. The geometric parameters of the eclipse can be converged to fit the observed line-strength variations like in the standard procedure of light-curve solution. However, despite such a procedure is a significant improvement compared to the standard methods, it is still limited by several assumptions, which are never exactly satisfied.

2.4.5 Disentangling with intrinsic line-profile variations

In view of the fact that components of binaries are often subjected to different kinds of variations and asymmetries (already mentioned ellipticity, reflection, spots, radial as well as nonradial pulsations), which are manifested as line-profile variations, the method of disentangling needs a further generalization. If some of these effects becomes non-negligible, the basic equation (11) must replaced by a more detailed expression

$$I(x,t) = \sum_{j=1}^{n} \int_s \mu I_j(x,s,\mu,t) * \delta(x - v_j(s,t)) d^2 s, \quad (48)$$

for the spectral flux as integral of monochromatic intensities over the visible parts of surfaces s of individual components j, each one Doppler shifted according to the local radial velocity, which can reflect now not only the orbital motion, but also rotation and pulsation of the stellar atmosphere. The unknown functions I_j depend now on a larger number of variables than the observed spectra on the left-hand side, equally as the velocities v_j. Consequently these functions cannot be reconstructed from the observed spectra without some additional conditions like it was

in the previous case of surface homogeneity. Such a condition can be based either on some geometric or physical assumption. For a suitable choice of some sets of functions for I_j and v_j, their free parameters can be adjusted to fit the observed spectra. However, it must not be forgotten that the solution is model dependent and that in principle it cannot be excluded that some other model may fit the data equally well or even better.

Quite generally the local intensity can be a linear combination of a few spectral functions I_j^k

$$I_j(x,s,\mu,t) = \sum_k f_j^k(s,\mu,t) I_j^k(x) \quad (49)$$

with coefficients f_j^k whose dependence on the position on the star-surface s, directional cosine μ and time t can be modelled up to a few free parameters. Substituting this into Eq. (48) we arrive at equation

$$I(x,t) = \sum_{j,k} I_j^k(x) * \Delta_j^k(x,t,p) , \quad (50)$$

which is formally identical with (13), apart of the fact that each component j can be now characterized by several spectra $I_j^k(x)$ (e.g. corresponding to different terms in the expression (41) for the limb darkening, or to spectra inside and outside a spot etc.) with different spectral broadenings

$$\Delta_j^k(x,t,p) = \int_s \mu f_j^k(s,\mu,t)\delta(x - v_j(s,t)) d^2 s . \quad (51)$$

Differences in these broadenings can ensure that the corresponding spectral functions can be decomposed from the observations using the general procedure described in Section 2.4.1.

2.4.6 Broadening by pulsations

One of the simplest generalizations of disentangling for a case of intrinsic line-profile variations, which was

outlined in the Section 2.4.5, is the problem of pulsating stars. Suppose first, that the atmosphere of a spherical star moves as a whole radially (with respect to its center) with instantaneous velocity $v_p(t)$. In agreement with conclusion (47) let us simplify the sum (49) to a single term linear in the directional cosine $\mu = \cos\vartheta$, which is a function of the projected distance $r = R\sin\vartheta$ from the centre of stellar disk

$$I_j(x, s, \mu, t) = s_j\mu\, I_j(x)\ .\qquad(52)$$

The total velocity of a projected surface element $\mu d^2 s = rdrd\varphi$ is the velocity $v_j(t)$ of the star as before, plus projection μv_p of the pulsational motion into the line of sight. The broadening function given by (51) thus reads[15]

$$\Delta_j(x, t_l, p) = 2\pi s_{jl}\int \mu\delta(x - v_j(t_l) - \mu v_p(t_l))rdr =$$
$$= \frac{2\pi R^2 s_{jl}}{v_p^3(t)}\left[(x - v_j(t_l))^2\right]_{x\in(v_j, v_j + v_p)}\ .\quad(53)$$

Its Fourier transform reads

$$\tilde{\Delta}_j(x, t_l, p) = \frac{2\pi i R^2}{v_p^3(t_l)}s_{jl}e_{jl}y^{-3}\qquad(54)$$
$$.\left[\exp(iyv_p(t_l))(2 - 2iyv_p - y^2v_p^2) - 2\right]\ ,$$

it means, that in comparison with Eqs. (23) and (27) it contains now also additional broadening terms corresponding to the line-profile variations.

Similar generalization can be done also for rotational broadening which causes LPVs in elliptic variables and can thus be found in the data. Non-zero limb-darkening leads in this case to asymmetry of lines and it complicates substantially the expression for Δ and its Fourier transform, equally as in the case of non-radial pulsations. However, Δ can be modelled and $\tilde{\Delta}$ calculated numerically in these cases.

2.5 Normalization of disentangled spectra

Let us investigate now in detail the obstacle of the decomposition, which was already mentioned in Section 2.4.2 on page 21 and which is immediately obvious from Eq. (12). If we choose $y = 0$, the equation (12) received for the integral mean values $\int I_j dx$ reduces to a singular system of linear equations

$$\tilde{I}(0, t) = \sum_{j=1}^{n}\tilde{I}_j(0)\ .\qquad(55)$$

According to the assumption of invariability of I_j in the simple disentangling, the mean intensity on the left-hand side of this equation should not depend on the time t. Assuming such a dependence to be caused only by a noise in individual exposures, the left-hand side can be replaced by its mean value, as it is done in Eq. (25). However, instead of a set of equations determining uniquely the other Fourier modes of component spectra, we have then this single condition restricting solutions for n values $\tilde{I}_j(0)|_{j=1}^{n}$ only to an infinite $(n-1)$-parametric set. In words it means that constant parts (continua) of the spectra cannot be decomposed, because they are invariant with respect to the Doppler shift. The continuum is never constant in the whole range of frequencies, so that in principle it should be possible to decompose the spectrum completely if it were to be available in the whole range of x with an unlimited precision. From the mathematical point of view it would require the use of additional conditions for limits, $\lim_{x\to\pm\infty} I(x, t) = 0$. In practice the whole spectrum is never available and its precision is insufficient to determine the Doppler shifts of continua.[16] Usually we decompose limited parts $x \in (x_1, x_2)$ of the whole spectrum which are rectified with respect to the local continuum. For these intervals the mean intensities

$$\tilde{I}_j(0) \equiv \langle I_j\rangle \equiv \int_{x_1}^{x_2} I_j(x)\frac{dx}{x_2 - x_1}\qquad(56)$$

differ from the individual continua C_j. These differences can be found by a new rectification of the decomposed spectra, however the ratios of values C_j must be estimated from some additional information.[17] The uncertainty of C_j is also why KOREL gives the disentangled component spectra I_j on its output only relatively, i.e. in the same units used at input and with an unknown shift of the zero level (and of the continuum). Because the input spectra for disentangling are supposed to be rectified with respect to the total continuum (or a pseudocontinuum)

$$C \equiv \sum_{j=1}^{n} C_j = 1\ ,\qquad(57)$$

the output

$$I'_j(x) = I_j(x) - \langle I_j\rangle + 1\qquad(58)$$

---

[15]Here we use the relation $rdr = -R^2\mu d\mu$. The bracket [ ] in (53) means that the quadratic function inside is multiplied by the characteristic function of the interval in subscript (or interval $(v_j + v_p, v_j)$ if $v_p < 0$), i.e. by 1 inside and 0 outside the interval. Note that if the intensity in the lines is taken to be homogeneous instead of (47), the pulsational broadening is linear instead of quadratic and it thus leads to a smaller amplitude of observed pulsational Doppler shifts.

[16]In fact just such an overestimation of the effect was a shortcoming of the historical paper by Christian Doppler 'Ueber das farbige Licht der Doppelsterne...' which he wrote and published in Prague in 1842.

[17]As it has been mentioned already in Section 2.4.2, the sets of linear equations (12) may be nearly singular also for some other low harmonics and due to the limited precision of the source data their solution may be unstable, especially if the RVs are not yet well converged. This results in some long-period waves on the decomposed spectra, which are frequently met during the procedure of convergence of the disentangling. Usually these waves disappear when a better solution is reached, however, a better rectification of the input spectra can also help.

is shifted for this value $C = 1$ to prevent negative values in absorption lines and to give an approximate information about the depths of the lines of individual components. However, to enable a comparison of the disentangled spectra with theoretical spectra from model atmospheres it would be desirable to calculate the component spectra rectified with respect to their (unknown) individual continua C_j, i.e. to find the functions $I_j(x)/C_j$.

The only value we can calculate from the input spectra is the total mean intensity

$$\langle I \rangle = \sum_{j=1}^n \langle I_j \rangle \ . \tag{59}$$

This value (which is decreased below the level of total continuum for the ratio of sum of equivalent widths of lines in the spectral region and the length of the region) is given at the output of KOREL for each spectral region. Even if we know, e.g. from a broadband photometry, the ratio of colour luminosities

$$L_j = \int I_j(x)\phi(x)dx \tag{60}$$

of the components, it does not tell us directly the ratio of $\langle I_j \rangle$, because L_j are integrated over a broader region with wavelength-dependent sensitivity ϕ of the photometric channels (given by filters/detectors). Both integrals (56) and (60) are decreased with respect to the levels of continua C_j by the sum of equivalent widths of absorption spectral lines contained in the corresponding region. However, for disentangling we usually choose narrow neighborhoods of strong (mostly absorption) lines, so that the values of $\langle I_j \rangle$ can be expected to be sensibly smaller in comparison with levels of continua C_j, while the photometric luminosities can nearly reach the values of integrals of the continua[18]

$$\langle I_j \rangle < C_j \ , \qquad\qquad L_j \le C_j \ . \tag{61}$$

Fortunately, the shifts of components' mean intensities with respect to their continua can be determined from the output disentangled spectra

$$\Delta_j \equiv C_j - \langle I_j \rangle = [I_j'(x) - 1]_{x \in cont.} \tag{62}$$

(cf. Eq. (58)) simply by fitting the level of continuum in I_j'. These n values should satisfy the bounding condition which follows from Eqs. (57) and (59),

$$Q \equiv 1 - \langle I \rangle - \sum_{j=1}^n \Delta_j = 0 \ , \tag{63}$$

the right-hand side of which is given at the output of KOREL as the integral of the input spectra. Neglecting this condition, the continuum shift of each disentangled component spectrum could be calculated independently by a new rectification of the output as its mean value in the continuum. Such a result could be then substituted into Eq. (63) to check it precision. An alternative approach is to solve for all Δ_j simultaneously by minimizing the sum

$$S \equiv \sum_j w_j \int [I_j'(x) - 1 - \Delta_j]^2 \tag{64}$$

with the condition (63). Here the weight w_j of each component spectrum can be chosen inversely proportionally to the square of its noise. The minimization can be done using the standard Lagrange multipliers method, i.e. solving the set of linear equations

$$0 = \frac{\partial}{\partial \Delta_j}[S - \lambda Q] = 2w_j \int [\Delta_j + 1 - I_j'(x)] - \lambda \ . \tag{65}$$

The solution reads

$$\Delta_j = \left(\int [I_j'(x) - 1] + \frac{\lambda}{2w_j} \right) / \int 1 \ , \tag{66}$$

where

$$\lambda \sum_j \frac{1}{2w_j} = [1 - \langle I \rangle] \int 1 - \sum_j \int [I_j'(x) - 1] \ . \tag{67}$$

Once the shifts Δ_j are determined (and continua C_j chosen), the rectified component spectra can be calculated according to

$$I_j(x)/C_j = 1 + (I_j'(x) - 1 - \Delta_j)/C_j \ . \tag{68}$$

Note, that a telluric component contributes also by its Δ_j, despite it has $C_j \equiv 0$ (but its $\langle I_j \rangle < 0$). It is natural to let the telluric lines be normalized with respect to the total continuum C.

3 Numerical method

The Fourier transform is calculated in KOREL using the procedure Fast Fourier Transform (FFT). Consequently, the input spectra must be discretized into 2^n points equidistant in logarithmic wavelength.[19] The shift ($v_j(t)$) of δ-function in Eq. (11) or its generalizations must be discretized with the sampling frequency (to give the function $\exp(iyv_j(t))$ in Eq. (12) periodic with the period of the data interval). Consequently, both $v_j(t)$ as well as the minimized sum S given by Eq. (19) are step functions (in t and p, resp.) in the

---

[18]The correction could be obtained from model atmospheres. In the next we will thus suppose that we know the ratio of the continua C_j from the photometry.

[19]The number of data points in each spectral region is 256 in the PC-version or its multiple by a power of 2 in the workstation version of the code KOREL.

numerical representation. To achieve a good resolution in velocity, it can thus be advantageous to interpolate the input spectra into higher sampling density than the original one read from the detector. The Fourier transforms of these spectra must be stored in the computer memory in the course of the solution. To enable the use of large number of spectra with high resolution, the spectra can be represented by several spectral regions only (containing spectral lines chosen for the solution), each one characterized by the initial wavelength and step in radial velocity per one bin. For each spectral region the functions S are calculated according to Eq. (19) and the corresponding sets of Eqs. (28) are independent. The total S summed over spectral regions is calculated only for the purpose of convergence of parameters p.

The spectra are supposed to originate from a multiple stellar system with a hierarchical structure shown in Fig. 5, where the numbers in circles are indexes of the star position, numbers in parenthesis give indexes of the corresponding orbit. The occupation of each position by a visible component is to be given by special key on input. The orbits Nos. 1, 2 and 3 can be suppressed by the choice of the corresponding period equal to 0.

The radial velocity of a component is thus given by

$$v_j(t; p) = \sum_o K(\cos(\omega + v) + e \cos \omega) , \qquad (69)$$

where the summation is performed over the orbits influencing the motion of the star (e.g. orbits Nos. 0, 2 and 3 for the star No. 1; note that the γ-velocity of the system does not appear in this formula – it can be specified only after the identification of lines in the component spectra). The true anomaly v is calculated according to

$$v = 2 \mathrm{arctg} \left(\sqrt{\frac{1+e}{1-e}} \mathrm{tg} \frac{E}{2} \right) \qquad (70)$$

from the solution of Kepler's equation

$$2\pi \frac{t - t_0 - \Delta t}{P} \left(1 - \frac{\dot{P}}{2} \frac{t - t_0 - \Delta t}{P} \right) = M = \qquad (71)$$
$$= E - e \sin E$$

for the time t corrected by

$$\Delta t = \sum_o \frac{PK}{2\pi c} (1 - e^2)^{3/2} \frac{\sin(\omega + v)}{1 + e \cos(v)} , \qquad (72)$$

for the light-time effect due to the higher orbits in the hierarchical system (e.g. orbits Nos. 2 and 3 for stars Nos. 1 and 2). The pericenter longitude is given by

$$\omega = \omega_0 + \dot{\omega}(t - t_0 - \Delta t) , \qquad (73)$$

i.e., the secular periastron advance (linear in time) can be taken into account. Similarly

$$e = e_0 + \dot{e}(t - t_0 - \Delta t) , \qquad (74)$$
$$K = K_0 + \dot{K}(t - t_0 - \Delta t) , \qquad (75)$$
$$q = q_0 + \dot{q}(t - t_0 - \Delta t) , \qquad (76)$$

The spectra and times of exposures are usually transformed into the heliocentric system. If not, the higher orbit can be used to make the corresponding correction. The secondary component of this 'solar' orbit can be used to remove the telluric lines (in an approximation) from the stellar spectra.

The minimization of S with respect to p is performed by the simplex method adapted from Kallrath and Linnell (1987).[20] Several orbital elements (cf. Table I), line strengths[21] or radial velocities[22] can be chosen from all of them for convergence in one step, the others being fixed. In each of these 'large' steps, there are performed many simplex transformations. The number of these 'small steps' is $10\times$ the number of the iterated parameters (at maximum 10 parameters can be converged in one large step). The actual status of the iteration is displayed on the screen (in order: No., code of simplex transformation, No. of the worst simplex point, value of S in this point and its values of parameters, i.e. in the same way as in FOTEL). At each simplex step the spectral decomposition is performed first, and then the line-strengths are calculated (if it is required by the corresponding key of the star). The self-consistent solution requires either to repeat these steps, or to store the values of line-strengths appropriate to the set of orbital parameters at a particular simplex point. The former approach is used in the present version of KOREL because the later would be memory exhausting. To find an exact self-consistent solution in each step would be very time consuming, hence only up to 5 iterations of successive spectra decomposition and line-strengths calculations are performed. The solution with free line-strengths is usually more sensitive to local minima in the basic parameters. To prevent this disadvantage it is recommended to hold the line-strengths fixed during the simplex solution (unless it is only tiny tuning of an already found solution) and to improve them in a subsequent step. Another possibility is to include some line-strengths (of chosen components in chosen exposure – e.g. very strong telluric lines or components participating in an eclipse)

---

[20] For details see description of the code FOTEL (Hadrava 2004b in this volume), where the same procedure is used.

[21] Note that either all line strengths for a chosen component can be calculated using the method described in Section 2.4.3, or only several of them (e.g. in exposures suspicious to be taken during an eclipse) using the simplex method.

[22] For a component which is not tied to an orbital motion – cf. *KEY* explained in Section 4.2.
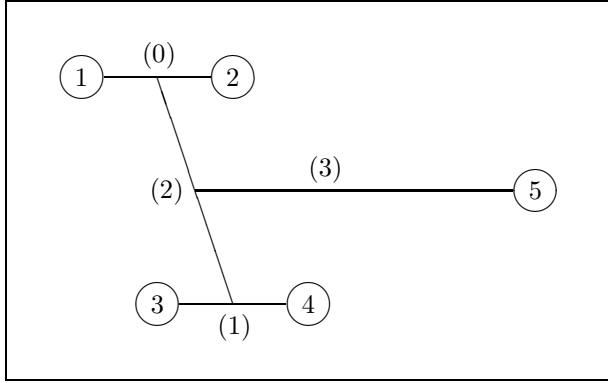
Fig. 5. The hierarchical structure of the stellar system. The numbering of component stars (in circles) and their orbits (in parenthesis) as used in KOREL is shown.

between the parameters converged by simplex with other line-strengths held fixed.

For the purpose of different numerical tests, there is built-in into KOREL a possibility to produce synthesized data with chosen orbital parameters. The profiles of each component can be then chosen in one of two types, either with broad wings (type 1)

$$I_j = -c\frac{\Delta^2}{(x-x_0)^2 + \Delta^2} \, , \tag{77}$$

or with continuum (type 2)

$$I_j = c\min\left[0, \left(\frac{(x-x_0)^2}{\Delta^2} - 1\right)\right] \, . \tag{78}$$

Random noise of a chosen amplitude can be added into each bin.

4 User's manual

4.1 Implementation of the code

The code KOREL is written in FORTRAN 77. It's PC-version (KOREL.FOR) includes on-line graphics (the package PHG.FOR), which is written for Micro-Soft-fortran. The larger LINUX-version (KOREL.F) contains analogous package with graphical output to files (HPGL- or PS-) only and could thus be compiled by any fortran compiler. Starting from release of May 2004 the LINUX-version needs also the file KOREL-PAR.F, where the maximum number of spectra nsp and pixels (bins) npx are given as parameters. Note that $npx2 = 2*npx$ is also required as the array dimension for the complex representation of Fourier transforms of the spectra.

The code PREKOR for preparing the data for KO-REL exists only in MS-version, because the use of on-line graphics is crucial for its use.

4.2 Controlling the run (file KOREL.PAR)

KOREL is controlled by the file KOREL.PAR, from which there are read (in free format, implicit fortran

definition of type is valid):

1. Control keys

$$KEY(j)|_{j=1}^5, K0, IFIL, KR, KPR \, .$$

- Key $KEY(j)$ defines if the lines of the star No. j (according to Fig. 5) are present in the spectrum ($KEY(j) \geq 1$) or not. If $KEY(j)$ is split into digits $KEY(j) = 10 \times K_1 + K_0$, then $K_0 = 1$ means that the line-strength of the component j is fixed, while $K_0 = 2$ means that the intensity of this component is to be solved according to Eq. (30). $K_1 = 0$ means that the radial velocities of the component j are subjected to the orbital motion according to Eq. (69), while $K_1 = 1$ means that its radial velocities are free parameters, either fixed or converged.
- Key $K0$ specifies if there should be read data from the file KOREL.DAT ($K0 > 0$), or if the calculation should go on with the previous data ($K0 = 0$), or (for $K0 < 0$) the number ($-K0$) of spectra is to be simulated.
- $IFIL$ is the number of harmonics to be removed by filtering.
- KR is the key of the form of graphic output PHG.OUT ($KR = 0 \Rightarrow$ no output, $KR = 1 \Rightarrow$ PCX-format, $KR = 2 \Rightarrow$ PostScript-format).
- KPR controls the level of output. The value of KPR is to be split into digits, $KPR = 10 \times KPR_1 + KPR_0$. Then $KPR_0 > 1$ specifies that the information on simplex convergence has to be printed also into the file KOREL.RES. $KPR_1 > 0$ specifies that the file KOREL.O–C has to be created, into which the difference spectra O – C will be written in the wavelength scale connected with the star No. KPR_1 (or in the original wavelength scale if $KPR_1 > 5$).

Table I. Numbering of orbital elements

i		orbital element
1	P	period [in days]
2	t_0	time of periastron passage [in days]
3	e	eccentricity
4	ω	periastron longitude [in degrees]
5	K	semiamplitude of radial velocity of the component with the lower index [in km/s]
6	q	the mass ratio of the component with the higher to that with the lower index
7	$\dot{\omega}$	the rate of periastron advance [in degrees/day]
8	$\dot{P}$	the time derivative of the period
9	$\dot{e}$	the time derivative of the eccentricity [in day^{-1}]
10	$\dot{K}$	the time derivative of K-velocity [in km/s/day]
11	$\dot{q}$	the time derivative of mass ratio [in day^{-1}]

2. Next, there is read (in a loop stopped by a line of zeros – like in FOTEL) information on the individual elements. In the PC-version or in the old LINUX-version (up to release of the year 2002) it has the form:

$$n, Kc, L1, L2, EL(n), \Delta(n) .$$

- n is the number of the element. For $n = 10\,j+i \leq 37$, n refers to the orbital element $i \mid_{i=1}^{7}$ (see Table I) of the orbit No. $j \mid_{j=0}^{3}$ (cf. Fig. 5); For $n = 100\,j + i \in (100, 600)$ it denotes the natural logarithm[23] of the line-strengths of the jth component (or telluric lines) in the ith spectrum, $EL(n) = \ln s_{ji}$. For $n = 1000\,j + i > 1000$ it means the radial velocity of the component j in the ith spectrum (for the case $KEY(j) \geq 11$).
- $Kc > 0$ specifies if the element No. n is to be converged. The maximum of Kc for all elements gives the number of large iteration steps.
- Keys $L1$, $L2$ specify if the (initial) values of the element and its step are to be read.
- $EL(n)$ and $\Delta(n)$ are the value of the element and its step (some numbers must be present even if they are ignored due to $L1 = 0$ and/or $L2 = 0$).

Because the above given coding of n limited the number of exposures to 99, a new format has been introduced to the LINUX-version, starting with release of 2003. It has the form:

$$c, j, i, Kc, L1, L2, EL(j, i), \Delta(j, i) .$$

---

[23]This natural-logarithmic scale of strengths is close to the traditional magnitude-scale (because $\ln x \simeq 0.434 \times \log x$), however, a more positive value means a more intensive contribution of the component spectrum. These logarithmic values are normalized on output in their exponentials, i.e. $\sum_l s_{jl} = \sum_l 1$ (such a normalization in intensities seems to be more stable than that in (pseudo-)magnitudes, $\sum_l \ln s_{jl} = 0$, used in KOREL up to year 2002).

Here the character c is equal either to 'o', 's', 'v' or 'w' and it distinguishes the kind of parameter EL labeled by indices i and j. The letter 'o' stands for orbital parameter number 'i' of orbit 'j' (i.e. it corresponds to the above explained case $n \leq 37$ in the PC-version, however, i may be higher here – cf. Table I). Letter 's' denotes the strength of lines of component j in the exposure number i (which, unlike the previous case $100 < n < 600$, may run over 100 up to the limit given by dimension of the corresponding arrays in KORELPAR.F). Similarly, 'v' denotes the velocity of component j in exposure i and 'w' enables to change the weight of exposure i (j being ignored). The output of these parameters has the same form in the new versions of the code (with explanation of meaning of the parameters at right on each line), so that the output values can be cut from KOREL.RES and copied to the input file KOREL.PAR for next run of the code.

3. If $K0 < 0$ then there are next read $-K0$ values of time, for which the data should be simulated. Next there must be given for each visible component its central intensity c, its width Δ [km/s] and the code 1 or 2 specifying if the profile should be given by Eq. (77) or (78). Finally the noise of the spectrum and RV/bin is read for the simulated data.

An example of KOREL.PAR for the LINUX version shown in Fig. 6 will thus converge periastron epoch (identical with max. of RV) and $K_{1,2}$ of a two-component binary (on circular orbit with period 1.234567 days) and solve for strengths of telluric lines (without filtering, with PS- output graphics and a detailed output protocol).

```
1 1 0 0 2 1 0 2 2 | key(1,...,5), k= Nr.  of sp., filter, plot, print
o 0 1 0 1 1 1.234567 0.000001 | sum= 9.8765
o 0 2 1 1 1 50001.000 .1 |
o 0 3 0 1 1 0.00 .1 |
o 0 4 0 1 1 90.00 1.  |
o 0 5 1 1 1 120.0 .5 |
o 0 6 1 1 1 .5 .1 |
o 3 1 0 1 1 365.256360000 0.100 = PERIOD(3)
o 3 2 0 1 1 51547.520600000 10.000 = PERIASTRON EPOCH
o 3 3 0 1 1 0.016710220 0.001 = ECCENTRICITY
o 3 4 0 1 1 301.795199910 10.000 = PERIASTRON LONG.
o 3 5 0 1 1 0.001000000 0.000 = K1
o 3 6 0 1 1 0.000038185 0.000 = M2/M1, K2 = 26.188293833
o 3 7 0 1 1 0.000009111 0.000 = d omega/dt
o 3 8 0 1 1 0.000000000 0.100 = d P/dt
s 5 1 0 1 1 -0.15890 0.10000
s 5 2 0 1 1 0.07530 0.10000
s 5 3 0 1 1 0.10141 0.10000
s 5 4 0 1 1 0.20137 0.10000
s 5 5 0 1 1 0.18172 0.10000
s 5 6 0 1 1 0.04557 0.10000
s 5 7 0 1 1 0.05994 0.10000
s 5 8 0 1 1 -0.10638 0.10000
s 5 9 0 1 1 -0.17056 0.10000
x 0 0 0 0 0 0 0 | end of elements
```

Fig. 6. Example of file KOREL.PAR.

4.3   Input data (file KOREL.DAT)

In the file KOREL.DAT there is read the time [in Julian dates], initial wavelength [in Å], RV per one bin [in km/s], the weight of each spectrum and (starting from release of 2003) also the number npx of pixels (bins) in each exposure.[24] It must be the same for all exposures and equal to 256 for the PC-version, while for the Unix-version it can be any multiple of 256 by number of the form 2^n, $n \geq 0$, up to the maximum value of npx defined by the parameter npx in the file KORELPAR.F. Next, there follow npx intensities in points with constant step in RV. There can be read at maximum 27 input spectra for the PC-version or any number up to nsp defined in KORELPAR.F for the LINUX-version. These spectra are to be given in up to mnu spectral regions ($mnu = 5$ in the PC-version), each region being characterized by the initial λ and by the step RV/bin. Naturally, the number of input spectra in each region and their phase distribution must be sufficient for their decomposition, i.e. it must at least higher (or equal) than the number of calculated components. The number of decomposed spectra, i.e. the product of number of spectral regions

× number of components must not exceed the value $mnsu$ given together with npx, nsp and mnu in the file KORELPAR.F (or fixed to 15 in the PC-version).

The file KOREL.DAT can be prepared by the code PREKOR.

4.4   The code PREKOR

The code PREKOR has been developed to facilitate the preparation of data for KOREL, it means to cut the proper spectral regions from a set of input spectra, to interpolate them into the equidistant logarithmic wavelength scale and to write them in the format required by KOREL in the file KOREL.DAT. Because a visual check of the proper choice of spectral regions is welcome, the PREKOR is written in MS-FORTRAN only and the distributed exe-version has to be run under DOS, even if the data are intended for a LINUX-version of KOREL. A version of PREKOR with PG-PLOT graphics is in preparation, however some problems with input of binary data makes it platform-dependent. Users without access to DOS- (or WINDOWS-) computers have to produce the KOREL.DAT input using some other facilities (e.g. to select proper regions using MIDAS or IRAF and to rewrite them into the required format by some user-written code).

As an input, PREKOR needs a list of input spectra in file PREKOR.LST and it produces the data for KOREL in its (newly created) output file PREKOR.

---

[24]An often mistake of users was to run older versions of KOREL compiled for a fixed value of npx with data prepared for its different value. For this reason the value of npx is free in the newer LINUX versions, but it must be given in the data itself. The data without this value prepared by an older versions of PREKOR can be modified to the new form using the code 'KORTRANS.F' (cf. Section 4.7.

OUT, which has then to be renamed as KOREL.DAT. Versions of PREKOR starting from October 2001 enable also to prepare parameters for disentangling the telluric lines, in which case an input file PREKOR.PAR is needed and the output is written as PREKOR.RES.

When started, PREKOR asks the user at first to choose the mode of calculation (or the type of KOREL data to be got). The choice of $mode = 0$ performs the above mentioned calculation of parameters for disentangling of telluric lines. The choice $mode > 0$ means to prepare data with the number $npx = 128 \times 2^{mode}$ bins in each spectral region. It means that $mode = 1$ is required for the PC-version of KOREL, $mode = 2$ for the older LINUX-version and both or some higher integer number (up to a limit given by the array dimensions in the PREKOR code) can be chosen for the version with KORELPAR.F-file.

For $mode > 0$, PREKOR reads the description of files with individual exposures from the file PREKOR.LST. Older versions of PREKOR stopped after finishing the work with the first 30 spectra from PREKOR.LST and a rearrangement of this input file was needed to continue with the subsequent spectra (and to concatenate the corresponding output PREKOR.OUT files). Starting from versions of January 2004, PREKOR continues to cut out from subsequent spectra the region chosen according to the first displayed spectra and offers them for saving into output.

The file PREKOR.LST must contain on each line the name of file with individual exposure, its Julian date, weight, a code of the type of data file and the value of its shift in RV's (in the format `a12,f11.4, f8.3,i2,f8.3`). If the weight is negative, the data file is ignored. The code equal to 0 denotes ASCI data files with wavelength and intensity in free format on each line. The code =1 refers to files *.RUI and 2 to *.UUI of data in format SPEFO used at Ondřejov observatory. The code =3 corresponds to the modified MIDAS output where the first three lines are a comment and then there follow lines with their sequence numbers (which are ignored by PREKOR), wavelengths and intensities. Tables produced by IRAF (with headings consisting of 106 records) can be read using the code =4. Finally, for the code =5, spectra in FITS- format ($BITPIX = -32$) can be read. The dimensions of arrays in the code limit the length of the input spectrum to 4100 bins at maximum (the rest is ignored). The only exception are the input files in the FITS-format (code =5) where the preview of the whole spectrum is drawn using averaged pixel-values and the data used for the calculations are then read only starting from the required wavelength (the limit of 4100 pixels is thus valid for the chosen spectral region only). The first spectrum is read

from its appropriate input file and its preview is plotted on the screen. User is asked to insert the initial wavelength and step in RV per bin. The corresponding spectral region is marked by a different colour on the wavelength scale and the chosen parts of spectra for the first portion of exposures (with non-negative weights) are then displayed to enable to check if their margins are really in the continuum. Recent versions of PREKOR enable also an approximate rectification of the chosen spectral region consisting in normalization by linear function joining the first and the last pixel of the region.[25] If the result is satisfactory, it can be saved into file PREKOR.OUT and subsequent spectral regions can be chosen in an infinite loop till the end of the run is not required.[26] The final file PREKOR.OUT can then be renamed and used as KOREL.DAT. The shift in RV of input spectra can be defined in the last column of PREKOR.LST either to transform the data from observed to heliocentric wavelength scale or to compensate for possible errors in wavelength-scale of the input spectra. These may be measured according to telluric lines either manually by some other mean or also by KOREL. A spectral region rich for telluric lines can be chosen first for this purpose and the column with O–C of RVs of telluric lines can be then copied from the file KOREL.RES into PREKOR.LST to reduce the scatter of RVs of telluric lines in other spectral regions.

The theoretical RVs of telluric lines can be predicted from the coordinates of the observed star. To calculate the corresponding fictitious orbital parameters of the telluric lines (usually taken as the component No. 5 on the orbit No. 3), PREKOR can be run in mod = 0. In this case an additional file PREKOR.PAR must be prepared in which are given (on separate lines) the right ascension and declination of the star (in hours and minutes or degrees and arc-minutes, resp.). On next line, the equinox of the source coordinates is read. The following line gives the geographic longitude and latitude of the telescope in degrees and its altitude above the sea level in meters. As a result, a block of lines with orbital parameters of the orbit are written into the file PREKOR.RES, from where they can be directly copied into KOREL.PAR. In addition, radial velocities of the telluric lines are calculated for each exposure listed in PREKOR.LST with higher precision taking into account also the planetary perturbations

---

[25]This option can help for quick inspection of non-rectified spectra by preventing the jumps between the margins of the regions. However, its use may be dangerous because of hiding possible spectral lines on margins and because of the influence of random noise in the ultimate pixels. A thorough rectification of the whole spectrum before the run of PREKOR is always preferable.

[26]The commands for controlling the run of PREKOR differ depending on version, but they are always displayed on the screen and offered to the user.

and the rotation of the Earth.

4.5 Outputs of KOREL

There are several possible forms of output. During the run of the code a basic information is shown on the screen. In the PC-version this information includes graphical output on the screen. Simultaneously, the figure can be written into the file PHG. OUT.[27] Main information about the run and the results is contained in the file KOREL.RES. Residual spectra can be stored in the file KOREL.O–C.

After the input of the data and control keys, the basic information on the task (e.g. the number of data and number of parameters to be solved) is summarized on the screen. Then the input spectra are drawn in green colour (in the PC-version) subsequently from the top to the bottom of the screen. During the iteration of parameters, a protocol on the simplex procedure is shown on the screen and it can be directed also to KOREL.RES.[28] In this protocol, the first number indicates the step (running up to ten times the number of iterated parameters), letter A, B, C or D shows the type of simplex operation and the following number the worst point of the simplex (which is to be improved).[29] It is recommended to check if the first point is improved reasonably soon. The opposite may indicate that there was chosen a too large initial value of step of some parameter (usually of that, which is improved first). Next in the line is written the highest value of the minimized sum. It should be decreasing, however an increase is possible at the shrinkage operation indicated by D.[30] Next there are typed the values of converged parameters, which help to check the status of the convergence. After the end of the convergence, the disentangled line profiles are shown at the bottom of the screen in blue colour and their superpositions with velocities corresponding to the solution of orbital parameters are plotted in blue over the green input spectra. Finally, each spectrum is fitted by the superposition of disentangled profiles with RVs independent of the orbital parameters and the corresponding fit is drawn in red. The L-shaped line in the figure indicates the wavelength unit (100km/s) and the unit of intensity (0.1 of the continuum level).

The file KOREL.RES yields most of the information about the calculation and its results. First, there are summarized the values of parameters characterizing the input of the task like the number of spectra etc. Next, during the iteration, there is written in

each its step the number of the step, the value of the sum S of squares for the present values of orbital parameters, its value after recalculation of the strengths of lines and the mean error of the intensity. If the print-mode is ≥ 2, the protocol on the convergence by simplex-method is copied here as well. After the iteration, the orbital parameters are printed for each orbit with non-zero period. Next, all non-zero strengths of lines are printed together with the final values of their steps (which can be changed with respect to their input values if the corresponding parameters have been converged by simplex). Then the values of S are repeated once more. Next the spectra of individual components are printed (in the order of columns corresponding to the order of component stars). It must be kept in mind, that the values of continua of individual components are unknown, so that the depths of lines are normalized with respect to the sum all continua. The number 1.0 is added to each component spectrum to prevent the negative values in absorption profiles. Each spectral region is introduced by information on the number of exposures contributing to it and by the mean value of their shifts of continua. Finally, for each exposure the radial velocities found as the best superposition of the decomposed spectra are printed. The order of the components corresponds to the previously used order of the output spectra and, in addition, it is indicated by the number of the component. Each radial velocity is followed by the value of O–C, where C corresponds to the value according to the final values of orbital parameters.

4.6 The code KORNOR

To facilitate the normalization of spectra disentangled by KOREL a simple code named KORNOR has been written (in MS-Fortran). This code reads the parameters *par*, *mi*, *npx*, *nsp* and *kr* from the first line and $C_j|_{j=1}^{nsp}$ from the second line of the file KORNOR.PAR and the disentangled spectra cut out from the file KORNOR.DAT in the form of table $\lambda_i, I'_{1,i}, ..., I'_{nsp,i}|_{i=1}^{npx}$ (for each spectral region separately). KORNOR draws first these input spectra on the screen in pale colours and with the unknown continua shifts as they are received from KOREL (i.e. the mean intensity shifted to the level = 1). It also draws (in yellow colour) an example composed spectrum with zero Doppler shifts of components and the proper shift of the continuum given by the parameter *mi* which is the mean intensity given for each spectral region in the output of KOREL. The continuum is then identified in this spectrum and marked by red line at the level = 1. It is defined to be in frequencies where the spectrum differs from 1 for less than a multiple *par* (which has to be established by the method of trials and errors, but typically can be chosen around 0.2) of the noise of the

---

[27]To facilitate the next work with the graphics output, it is named PHG.PS in the case of PostScript format.

[28]Cf. the use of key *KPR* in Section 4.2.

[29]See the FOTEL-manual (Hadrava 2004b) for a more detailed explanation of the protocol and its meaning.

[30]Obviously, the monotonous decrease of the sum can also be violated by an insufficient convergence of the line strengths (as explained on page 3).

spectrum. At these points the integrals at continua of each component are calculated and the continuum shifts are found according to Eq. (66). The rectified component spectra are finally rescaled, i.e. calculated by Eq. (68) using continua values C_j given at the file KORNOR.PAR and they are drawn on the screen and written on the output.

4.7   The code KORTRANS

This code was originally written to transform the file KOREL.DAT from DOS to UNIX format on computers, where the utility DOS2UNIX is not available. The code PREKOR writes intensities for each exposure by one command – always 10 values in one line ended by mark nonunderstandable to UNIX. The code KORTRANS can read each line separately from these files renamed to KORTRANS.IN and to write them into KOREL.DAT directly readable by KOREL. Because the older version of KOREL did not require the number npx of bins in the heading of each exposure, KORTRANS can update the old data by inserting this value given in file KORTRANS.PAR. This file has a single line with values npx, v_1, v_2, Δv in a free format (e.g. "512 0.02 0.98 0.005"). If the value $dv > 0$, the spectral region of each input exposure is transformed (filtered or tapered at edges – Section 2.4.2, p. 22) according to formula

$$I_{out}(v) = 1 + \frac{I_{in}(v) - 1}{(1 + \exp \frac{v_1 - v}{\Delta v})(1 + \exp \frac{v - v_2}{\Delta v})} \ , \qquad (79)$$

where v is the logarithmic wavelength rescaled to be 0 and 1 on both edges of the spectral regions. This tapering suppresses smoothly (on a characteristic width Δv) spectral lines and deviations of continuum from 1 at edges of the spectral region (i.e. below v_1 and above v_2).

4.8   Problems with KOREL

In this Section some hints, explanations to problems and answers to often asked questions of users will be given.

Incomprehensible list input in korel.dat: This error message and abort at the beginning of the run of KOREL appears when the file KOREL.DAT is prepared by PREKOR on a DOS operating computer and it is transmitted to a LINUX operating computer for the run of KOREL. It is due to the incompatibility of the ends of lines between these systems. It can be corrected using the utility DOS2UNIX on the file KOREL.DAT or using the code KORTRANS, which can yield some additional corrections to the input data.

Array bounds exceeded in subroutine CSWAP: This subroutine is called to exchange two columns of a matrix in the solution of a set of linear equations

by the subroutine CGSEV accepted from the LAPACK package of FORTRAN routines. It uses a standard trick to speed up matrix operations avoiding the lengthy straightforward calculation of position in computer memory for each element of a multidimensional array by a use of its equivalence with a vector. The dimension of this vector is declared only formally in this subroutine (and it is underestimated) and the proper bound of the array is ensured by the correct demands of the higher subroutine. Array bounds checking of the FORTRAN compiler should thus be switch off.

Undulation of disentangled spectra: Sometimes it happens that the disentangled spectra have large amplitude and long wavelength wavy perturbations in antiphase (which cancel in the sum of all components). Such errors appear quite often at the beginning of the spectra decomposition and in favourable case (but not always) they are suppressed in the course of convergence of the orbital and other free parameters. This feature is due to a bad definition of lower Fourier modes by Eq. (19); the continua of components cannot be distinguished, because they are not affected by the orbital motion at all, and the lower modes are affected only slightly, hence they are determined only poorly — the corresponding matrix is nearly singular and a small error (e.g. in rectification of input spectra) can result in exagerrated values of amplitudes of the modes. This danger increases if the disentangled regions are long compared to the real RV- amplitudes. The contributions of these poorly determined modes to the total minimized sum S can be still small, so that the solution of higher Fourier modes and the free orbital and others parameters can be still correct. In such a case, it is sufficient to rectify the disentangled spectra once more.[31] However, there is a real danger that the RVs or line-strengths will converge to a false minimum in which the source of the low modes will be fitted best and the true spectral lines encrypted in higher modes will be ignored. Several actions can be undertaken to prevent this failure. Firstly, user should check if all exposures are correctly rectified[32] and either to improve or to remove suspicious exposures. The use of filtering out the lower modes (by the key $IFIL$ described in Section 4.2) may help to hit the proper solution, in which finally also the undulation may be suppressed. A better initial estimate of orbital parameters or line-strengths (e.g. from other spectral regions, from some other sources or simply found by chance from numerous trials) may also be helpful.

---

[31] A simultaneous rectification of all components at once with the condition of mutual cancelling of the corrections would be desirable.

[32] Problems may arise also from overlaps of orders in echelle spectra.

Acknowledgement

References

Bagnuolo W. G. Jr., Gies D. R.: 1991, ApJ 376, 266

Ferluga S., Floreano S., Mangiacapra D.: 1991, La Lettre de l'OHP 6, 3

Ferluga S., Floreano S., Bravar U., Bédalo C.: 1997, A&AS 121, 201-209

Hadrava P.: 1990, Contrib. Astron. Obs. Skal. Pl. 20, 23

Hadrava P.: 1991, "FOTEL – User's guide" (electronic document), Astron. Inst. ČSAV

Hadrava P.: 1995, A&AS 114, 393-396

Hadrava P.: 1997, A&AS 122, 581-584

Hadrava P.: 2001a, "The method of spectra disentangling and its links to Doppler tomography", in: *Astrotomography, indirect imaging methods in observational astronomy*, H. M. J. Boffin, D. Steeghs, J. Cuypers (eds.), Lecture notes in physics vol. 573, pp. 261-268, Springer

Hadrava P.: 2001b, "Spectroscopy of binaries", DSc. thesis (in Czech), Astronomical Institute ASCR, Ondřejov

Hadrava P.: 2003, "Spectroscopy of binary stars", in: *New directions for close binary studies: The royal road to stars*, O. Demircan, E. Budding (eds.), Publ. COMU Ap. Research Center, Vol. 3, pp. 84-90

Hadrava P.: 2004a, "Disentangling of spectra of multiple stars", in: *Spectroscopically and spatially resolving the components of the close binary stars*, R. W. Hilditch, H. Hensberge, K. Pavlovski (eds.), ASP. Conf. Ser. 318, pp. 86-94

Hadrava P.: 2004b, Publ. Astron. Inst. ASCR 92, 1

Hadrava P.: 2005, Astrophys. & Sp. Sc. 296, 239

Hadrava P., Kubát J.: 2003, "Limb Darkening and Line-profile Variations in Eclipsing Binaries", in: *Workshop on Stellar Atmosphere Modeling*, I. Hubeny, D. Mihalas, K. Werner (eds.), ASP Conf. Ser. 288, pp. 149-152

Hill G.: 1993, in: *New Frontiers in Binary Stars Research*, K.-C. Leung, I.-S. Nhu (eds.), ASP. Conf. Ser. 38, p. 127

Holmgren D.: 2004, ASP Conf. Ser. 318, p. 95

Hynes R. I., Maxted P.F.L.: 1998, A&A 331, 167

Ilijić S., Hensberge H., Pavlovski K.: 2001 "Fourier disentangling of composite spectra", in: *Astrotomography, indirect imaging methods in observational astronomy*, H. M. J. Boffin, D. Steeghs, J. Cuypers (eds.), Lecture notes in physics vol. 573, pp. 269-275, Springer

Kallrath J., Linnell A. P.: 1987, ApJ 313, 346

Kallrath J., Milone E. F.: 1999, Eclipsing binary stars: modeling and analysis, Springer-Verlag, New York, Berlin

Rucinski S.: 1992, AJ 104, 1968

Rucinski S.: 2002, AJ 124, 1746

Simkin S. M.: 1973, A&A 31, 129

Simon K. P., Sturm E.: 1994, A&A 281, 286

Simon K. P., Sturm E., Fiedler A.: 1994, A&A 292, 507

Škoda P.: 1996, in: *Astronomical Data Analysis Software and System V*, G. H. Jacoby, J. Barnes (eds.), ASP. Conf. Ser. 101, p. 187

Sturm E., Simon K. P.: 1994, A&A 282, 93

Zucker S., Mazeh T.: 1994, ApJ 420, 806

Zucker S., Torres G., Mazeh T.: 1995, ApJ 452, 863